

The Dynamic Analysis of the Backward Swimming Mode for Biomimetic Carangiform Robotic Fish

Chao Zhou, Zhiqiang Cao, Shuo Wang, Min Tan

Abstract—The swimming backward method for biomimetic carangiform robotic fish is analyzed in this paper based on the dynamic/kinematic model. The equation of Lagrange of multi-link carangiform robotic fish and simplified fluid force are induced to calculate the dynamic and kinematic characteristics of the motions. A specific gait is calculated to make the profile of the carangiform robotic fish's undulation fit the characteristics of European eel's swimming backward, which is summarized from the motion sequence of European eel. The simulated and experimental data is given to verify the method.

I. INTRODUCTION

THE robotic fish attracts many researches' attention. Many theories are proposed to explain the secrets of fish swimming mechanisms and summarize driving modes of fish motions, e.g. the large-amplitude elongated-body theory[1], the two-dimensional (2-D) waving plate theory[2][3], the jet formed behind the fish body[4], the 3-D waving plate theory (3DWDP)[5][6]. There are five kinds of fish motion according to the undulatory swimming movements [7]. Many prototypes of the biomimetic robotic fish have been developed by the inspired of the characteristics [8]-[16]. Generally speaking, biomimetic robotic fish is defined as a fish-like aquatic vehicle based on the swimming skills and anatomic structure of a fish: the undulatory/ oscillatory body motions, the highly controllable fins and the large aspect ratio lunate tail. On the view of the robotics, the ability of swimming backward is necessary. When the robotic fish is in some narrow pile or gap where it can't turn back, it needs some reliable methods for swimming out. Swimming backward is selected for this application, as a mean of maneuver, may play an important role in some special occasion.

In nature, only European eel can swim backward by the body and tail's undulation [7] [17], while all other fish swim backward slowly by the oscillation of pectoral fins. Some biomimetic robots are able to swim backward. Eel-like robots are often symmetrical between the head and tail. The robot eels swim backward when the undulation amplitude of the head is larger than that of the tail. A five-link eel-like robot is developed to implement several kinds of motion including

swimming backward [8]. Because the head link and the caudal link of the anguilliform robotic fish is symmetrical, the motion of swimming forward and backward is symmetrical and the swimming backward can be realized easily by exchanging the motion law of anterior links with the posterior ones. The structure of robotic fish with ribbon fin is similar to the robotic eel to a certain extent. Every fin can undulate free and symmetrical [9]. When the anterior fins undulate larger, the robot swims backward. These two kinds of robot are both symmetrical in structure, while many other underwater robots, based on bionic fins or multiple undulation fins, utilize the fins flapping forward or backward to make the robot swim forward or backward, just like fish's pectoral fins [10][11]. All these robots have the same hydrodynamic characteristic when swimming backward and forward.

However, carangiform fish motion's large amplitude undulation is mainly confined to the last 1/3 part of the body [5], which is much different from the eel. Although this difference endows the carangiform fish swim with high speed and high efficiency, the flexibility of the tail reduces and the head is not symmetrical with the tail. The carangiform robotic fish has the same characteristics, so simply reverse of the motion rule is not suitable for the carangiform robotic fish.

In this paper, the carangiform robotic fish is simplified to jointed plates. The kinematic model of this robotic fish is given to discuss the propulsion. The problem of swimming backward is attributed to the selection of gaits, which make the robotic fish's swimming profile fit the features of swimming backward of European eel. The gaits are searched according to the kinematic model, and the carangiform motion is modified according to it to realize the swimming backward.

The sense of the swimming backward motion for the carangiform robotic fish is that it diversifies the motions without changing neither the mechanical structure nor the advantage on propulsion, and it makes the robotic fish more flexible to accomplish complex maneuverable motion in swimming. It enhances the capability and adaptability of locomotion, and simplifies the design of robotic fish because pectoral fins are needless. It may be applied to the accurate location without large amplitude turning, the work in confined gaps, pipelines and maze etc. It enhances the capability and adaptability of locomotion and it is beyond the carangiform fish in nature at this point.

The rest of the paper is organized as follows. Section 2 discussed the robotic fish's model and the hydrodynamic force model. Section 3 given the description of the gaits calculation. Simulations and experiments are given in Section 4 and Section 5 concludes the paper.

Manuscript received Feb. 20, 2008. This work was supported in part by the NSFC (No. 60635010, No.60605026, No.60725309) and CASIA Innovation Fund for Young Scientists.

Chao Zhou is with Laboratory of Complex Systems and Intelligence Science, Institute of Automation Chinese Academy of Sciences, Beijing 100080, China (corresponding author to provide phone: 86-10-82614439; fax: 86-10-62560912; e-mail: zhouchao@compsys.ia.ac.cn).

Zhiqiang Cao, Shuo Wang, Min Tan are with Laboratory of Complex Systems and Intelligence Science, Institute of Automation Chinese Academy of Sciences, Beijing (e-mail: {zqcao; swang; tan}@compsys.ia.ac.cn).

II. MODELING OF THE ROBOTIC FISH

We hope the swimming backward method for European eel can be used to endow carangiform robotic fish with the ability of swimming backward, but the structure is much different. The flexibility of the tail reduces and the head is not symmetrical with the tail. Therefore, the result of this method for carangiform robotic fish may be unlike to for European eel. So the task of swimming backward is that a motion control law for robotic fish should be given to make the robotic fish swimming like the European eel. To deal with this problem, a dynamic model of our carangiform robotic fish is given to analyze the kinematics of freely swimming.

A. Carangiform robotic fish

Our carangiform robotic fish consists of three parts: stiff anterior body, flexible rear body and an oscillating lunete caudal fin. The well-streamlined rigid anterior body is passively side slipped to some extent, while the flexible rear body takes on significant lateral movements. The whole body of fish, from the perspective of mechanical engineering, can be designed as a multi-link mechanical structure, which consists of several oscillating hinge joints actuated by motors. This structure is a typical serial structure[12].

The swimming gaits for the multi-link mechanism should be calculated. For the purpose of describing the motion laws of the multi-links, the following method is adopted, which make the selection flexible. Assuming the fish have N links, $l_1 \dots l_N$, and the angles of joint, which are the angles between the l_i and l_{i+1} , are sine function [8]:

$$\phi_i(t) = A_i \sin(\omega t + \psi_i) \quad (1)$$

where A_i is the amplitude of i^{th} joint angle, ψ_i is the phase $i = 1 \dots N - 1$.

B. The simplify of the system

For the purpose of analyzing the motion effect, a motion model of robotic fish is required. This robotic fish is a typical serial robot in structure, and it can be described by the function of Lagrange, analogously. The robotic fish swims in the water freely, and the movement of links interacts with the water: the movement decides the amount and direction of the hydrodynamic forces and the forces also decide the fish's movement. The kinematic and dynamic problems are coupled, and they can not be calculated respectively. (1) is the relative motion law of links.

The basic idea for modeling the biomimetic robotic fish is to build the Lagrange's function unrelated with the internal force based on the structure of joints. The generalized forces got from the Lagrange's equation of the second kind are equal to the forces calculated according to the hydrodynamics. Finally, a system of partial differential equations can be built and the movement of the robotic fish is solved. Some reasonable assumptions are given to simplify the question:

a) The body of robotic fish can be treated as N plates jointed together[2] [8].

b) The robotic fish swims on still water, and it is not affected by the influence of reflection wave from the

environment.

c) The deformation of robotic fish can be ignored except the motion of the joints.

Motion of the robotic fish is analyzed only in two dimensions of the horizontal plane, which is the most valuable and representative situation in the propulsion.

The top view of the simplified multi-link structure is shown in Fig. 1 with useful parameters labeled under XOY , which is the world rectangular coordinate system (WRCS).

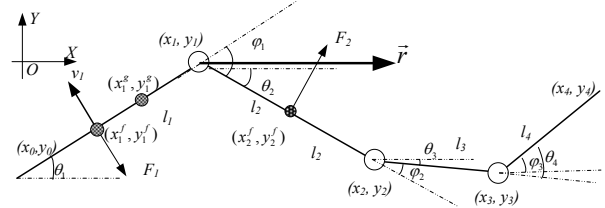


Fig. 1 The simplified robotic fish and some parameters definition

In the figure, l_i is the i^{th} link of robotic fish, and it also the length of the link. θ_i is the angle between i^{th} link and polar axis. ϕ_i is the angle between i^{th} link and extension line of $i-1^{th}$ link. The parameters θ_i , ϕ_i are both anti-clockwise positive. (x_i^f, y_i^f) , (x_i^g, y_i^g) and (x_i, y_i) are the center of figure, the center of gravity and the end point of i^{th} link, respectively. The joint angle ϕ_i is known, and it is (1) when the robotic fish is advancing.

C. Lagrangian Function of system

The potential energy is constant E . The kinetic energy of each link is the sum of the kinetic energy of translation under WRCS and the kinetic energy of rotation under the centre-of-mass system, so the Lagrange's function is defined as follows:

$$\begin{aligned} L &= \sum_{i=1}^N \frac{1}{2} m_i v_i^2 + \sum_{i=1}^N \frac{1}{2} I_i \omega_i^2 + E \\ &= \sum_{i=1}^N \frac{1}{2} m_i \left((\dot{x}_i^g)^2 + (\dot{y}_i^g)^2 \right) + \sum_{i=1}^N \frac{1}{2} I_i (\dot{\theta}_i)^2 + E \end{aligned} \quad (2)$$

where m_i is the mass of the i^{th} link. I_i is the moment of inertia of the i^{th} link under the centre-of-mass system.

x_1, y_1, θ_2 are selected as the generalized coordinate, and let $X = x_1, Y = y_1, \Theta = \theta_2$. l_i^g is labeled as the length between (x_i, y_i) and (x_i^g, y_i^g) , then we have:

$$\begin{cases} x_1^g = X - (l_1 - l_1^g) \cos \theta_1 & y_1^g = Y - (l_1 - l_1^g) \sin \theta_1 \\ x_2^g = X + l_2^g \cos \theta_2 & y_2^g = Y + l_2^g \sin \theta_2 \\ \theta_1 = \Theta - \phi_1 & \theta_2 = \Theta \\ x_i^g = X + \sum_{j=2}^{i-1} l_j \cos \theta_j + l_i^g \cos \theta_i & i \geq 3 \\ y_i^g = Y + \sum_{j=2}^{i-1} l_j \sin \theta_j + l_i^g \sin \theta_i & i \geq 3 \\ \theta_i = \Theta + \sum_{j=2}^{i-1} \phi_j & i \geq 3 \end{cases} \quad (3)$$

Rewrite the Lagrange's function with (3), and we can get $L = L(X, Y, \Theta)$.

D. The force and moment model

The hydrodynamic forces acting on the robotic fish are decided by the instantaneous movement. A hydrodynamic drag model is employed to analyze forces perpendicular to the surface of swimming robotic fish, which has been used extensively in the case of large Reynolds number in the literature [8][13][18], and it is:

$$F = -\mu \text{sgn}(v^\perp)(v^\perp)^2 \quad (4)$$

where $\mu = \rho CS/2$ is the drag coefficient, ρ is the density of water, C is shape coefficient, and S is effective area. v^\perp is the projection of the velocity along the direction perpendicular to the surface.

The forces acting on the robotic fish are divided to three parts: pressure on links, approach stream pressure and friction drag.

1) The pressure on links: the hydrodynamic force on the robotic fish's i^{th} link when it swings:

$$F_i^\perp = -\mu^\perp \text{sgn}(v_i^\perp) |v_i^\perp|^2 = -\mu^\perp v_i^\perp |v_i^\perp| \quad (5)$$

where F_i^\perp is the pressure on i^{th} link, v_i^\perp is the projection of the velocity of i^{th} link along the perpendicular direction, and μ^\perp is the drag coefficient with C of flat plate type [18].

$$v_i^\perp = \frac{dx_i^f}{dt} \sin \theta_i - \frac{dy_i^f}{dt} \cos \theta_i \quad (6)$$

where:

$$\begin{cases} x_1^f = X - (l_1 - l_1^f) \cos \theta_1 & y_1^f = Y - (l_1 - l_1^f) \sin \theta_1 \\ x_2^f = X + l_2^f \cos \theta_2 & y_2^f = Y + l_2^f \sin \theta_2 \\ x_i^f = X + \sum_{j=2}^{i-1} l_j \cos \theta_j + l_i^f \cos \theta_i & i \geq 3 \\ y_i^f = Y + \sum_{j=2}^{i-1} l_j \sin \theta_j + l_i^f \sin \theta_i & i \geq 3 \end{cases} \quad (7)$$

l_i^f is the length between (x_i, y_i) and (x_i^f, y_i^f) ,

2) The approach stream pressure: It is introduced because the water pushes on the cross section of the robotic fish when the robotic fish advances:

$$F_1^\parallel = -\mu^\parallel v_1^\parallel |v_1^\parallel| \quad (8)$$

where $v_1^\parallel = \dot{X} \cos \theta_1 + \dot{Y} \sin \theta_1$ is the projection of the velocity of first link along the parallel direction, and μ^\parallel is drag coefficient with the type of bullet [18]. Considering the cross-sectional area of the other link is smaller than the first, the flow's effect is reduced and $F_i^\parallel (i \geq 2)$ is ignored.

3) The friction drag: There is friction drag acting on the

surface of the robotic fish, which is parallel to the body. It is often evaluated empirically (30%-50% of the approach stream pressure). In this paper, we use 50% because of the unsmooth surface of the robotic fish.

$$F_f = 50\% F_1^\parallel = -\frac{u^\infty}{2} v_1^\parallel |v_1^\parallel| \quad (9)$$

Therefore, the composition of forces on the X-axis, Y-axis and the composition of moment act on the joint point (X, Y) can be obtained.

Based on (2) and (7)-(9), a system of partial differential equations of X, Y, Θ, t can be obtained:

$$\begin{cases} F_x = \frac{d}{dt} \frac{\partial L}{\partial \dot{X}} - \frac{\partial L}{\partial X} = \sum_{i=1}^N F_i^x + (F_1^\parallel + F_f) \cos \theta_1 \\ F_y = \frac{d}{dt} \frac{\partial L}{\partial \dot{Y}} - \frac{\partial L}{\partial Y} = \sum_{i=1}^N F_i^y + (F_1^\parallel + F_f) \sin \theta_1 \\ M_\Theta = \frac{d}{dt} \frac{\partial L}{\partial \dot{\Theta}} - \frac{\partial L}{\partial \Theta} = \sum_{i=1}^N [-F_i^x (y_i^f - Y)] + \sum_{i=1}^N F_i^y (x_i^f - X) \end{cases} \quad (10)$$

The movement of the robotic fish is described by $X(t), Y(t), \Theta(t)$, which are all determined by the tail's motion law $\varphi_i(t)$. The equations are complex, and they are solved by numerical method with boundary conditions at initial time.

III. THE GAITS FOR SWIMMING BACKWARD

The robotic fish's locomotion is decided by the motions of links (the link angle φ_i), which can be considered as gaits of robotic fish. The gait includes the amplitude and the phase of each link. The motion of the robotic fish may be considered and determined by the gaits regardless of body wave curve. A gait may be calculated to make the robotic fish's swimming profile fit the features of backward swimming of European eel.

A. The backward swimming of European eel

Most of fish swim backward by pectoral fins except European eel, which is a kind of Anguilliform mode. The European eel utilizes the body's undulation to swim backward.

In paper [17], Kristiaan D'Aout and Peter Aerts studied the kinematic characteristic of backward swimming in the European eel (*Anguilla anguilla*). Compared with forward, the backward swimming has two major kinematic differences. In the backward swimming, the slope of wave frequency against swimming speed is significantly higher, and the amplitude profile along the body of the propulsive wave is rather uniform along the body, which is similar to the tail-tip amplitude during forward swimming with values. An example is shown in Fig. 2. These conclusions give a feasible approach to implement the swimming backward for the carangiform robotic fish: if it undulates like the backward law of the European eel, it may swim backward.

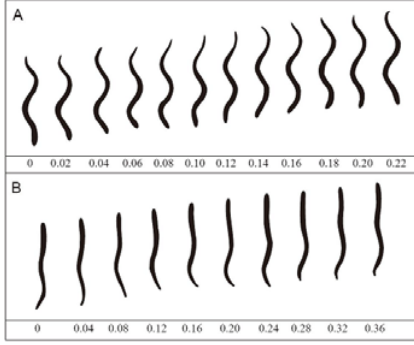


Fig. 2 Dorsal-view contour plots of approximately one cycle of backward (A) and forward (B) undulatory swimming in *Anguilla anguilla* [17]

The motion of swimming backward for European eel is not a simple reversion of swimming forward, and the body wave for swimming backward is not given in the paper [17], and we can summarize from Fig. 2 and the paper that:

- The oscillation amplitude of every segment is uniform, about 1/6 of body length, and it is larger than that of forward.
- The body wave number is larger, and about $k=1.5$.
- The wave frequency against swimming speed is significantly higher.



Fig. 3 The definition of reference frame $X_b O_b Y_b$

Therefore, under the frame $X_b O_b Y_b$ defined in Fig. 3, a form of sinusoidal function is adopted because it is widespread in experimental biology of fishes:

$$y_{body}(x, t) = A_{back} \sin[k(x - v_{back}t - \tau) + \omega t] \quad (11)$$

where A_{back} is the amplitude of the body undulation. v_{back} is the backward velocity of fish, τ is the initial position.

One important difference between (1) and (11) is that they are under different reference frame: (1) is under fish-body-fixed frame and (11) under inertial frame of reference. The undulation amplitude of the rostral part of the body during forward is very small and can be ignored, therefore (1) can be easily convert to control law of joint motors for robotic fish [12][15]. But the amplitude of rostral part during backward swimming is much larger, And (11) under WRCS, can not be convert to the gaits of every joints with the same method. The problem could be described as follows: a certain control law should be found that make the robotic fish's body profile fit the kinematic characteristics of swimming backward of European eel.

B. The gait calculation

Firstly, we solve (10). The head of robotic fish is assumed to point to the positive direction of X axis, and the position is at origin point at initial time. The Fig. 4 gives a simulation

result of forward swimming.

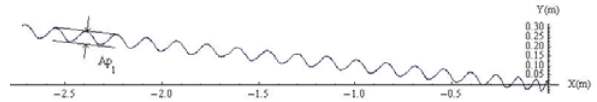


Fig. 4 Simulated data of forward motion, the trace of (X, Y).

We define Ap_i as the distains between the two envelope curves of the trace, which is the amplitude of (x_i, y_i) , as shown in Fig.4, and we can define Ap_i as the amplitude of (x_i, y_i) , $i = 1 \dots 3$, similarly.

Therefore, the amplitude of links' undulation should be uniform, and the phase should fit the body wave number. The gaits problem of swimming backward can be described as follows:

$$\begin{cases} |Ap_i - Au| \leq \delta \\ \psi_i = -k \sum_{j=2}^{i+1} l_j \end{cases} \quad (12)$$

where $Au = l/6$ (l is the total length of the robot body) and $k = 1.5$, δ is the approximate error.

The gaits can be got by searching the parameter space: $\{A_1\} \times \{A_2\} \times \{A_3\}$ to find a set $\{A_1^*, A_2^*, A_3^*\}$ fits (12).

IV. SIMULATIONS AND EXPERIMENTS

An experimental biomimetic robotic fish system is constructed based on the simplified carangiform propulsive model. Fig. 5 gives a prototype of the robotic fish. Parameters of the robotic fish prototype are shown in Table I.

TABLE I
PARAMETERS OF THE ROBOTIC FISH

Item	Value
Max size(L*W*H)(m)	0.390*0.054*0.086
Total weight(kg)	0.860
Max oscillating frequency(Hz)	2.78 (in water)
Body-wave constants	$c_1=0.05, c_2=0.09, k=0.5$
Max swimming velocity(m/s)	~0.42
$S_i(10^{-4}m)$	164, 36, 22, 48
$l_i(m)$	0.205, 0.055, 0.040, 0.080
$m_i(kg)$	0.705, 0.065, 0.045, 0.020
$I_i(10^{-3}kg \cdot m)$	246.9, 1.6, 0.6, 1.0

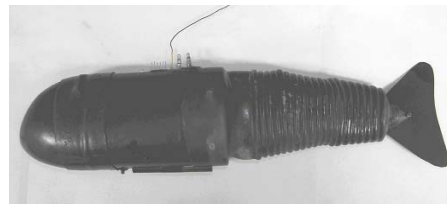


Fig. 5 Prototype of the robotic fish

A. Simulations of backward

Equation (12) is solved to obtain the gaits with $\delta = 2\%l$ and the motion is simulated. Fig. 6 shows a simulated trace of (x_i, y_i) with a feasible solution.

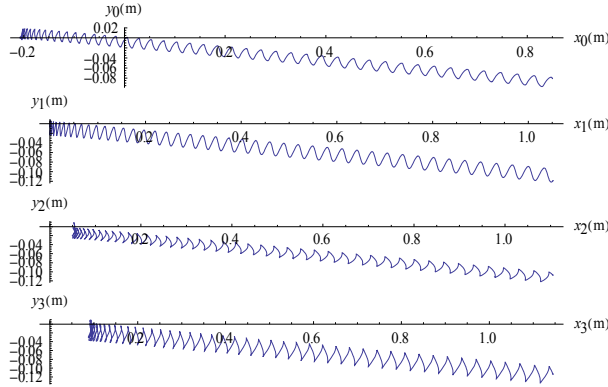


Fig. 6. Simulated data of backward motion. They are the trace of (x_i, y_i) , $i = 1 \dots 3$, respectively.

The orientation is not the direction that the robotic fish pointed to at initial time. It is because that forces acting on robotic fish are not symmetrical when it starts. The steady average velocity is -0.0519m/s , and the average velocity of every period at beginning is shown in Fig. 7.

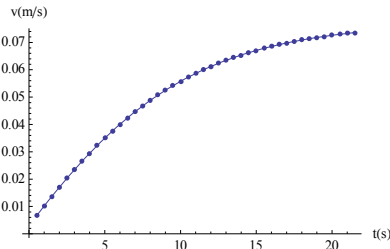


Fig. 7 Average velocity at every period

B. Experiments

Experiments are conducted in an experiment pool. An overhead camera is inducted to capture the video of the robotic fish motion and the video information is sent to the computer to recognize and record the realtime position.

Experiment 1: The relationship between the frequency and back swimming velocity

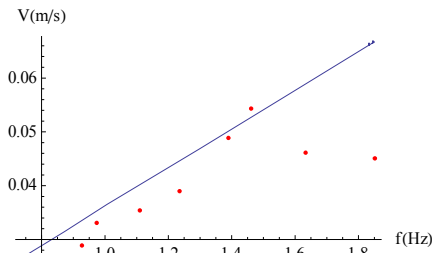


Fig. 8. The velocity at different frequency

The frequency of the tail oscillation is set from 0.5Hz to 2.78Hz . The results in Fig. 8 show that the dynamical and kinematical analysis and the gaits of motion are feasible.

From Fig. 8, the velocity reaches the highest at the frequency of $f=1.46\text{Hz}$, and $v_{\max}=0.0542\text{m/s}$. the robotic fish moves smoothly in the water when $f < 1.85\text{Hz}$, or else it will stagnate and become disorderly because the violent wave

destroys the hydrodynamic characteristic severely at a higher frequency. When the frequency is lower than 0.74Hz , the swimming backward is too slow to measure, which fits the feature c) of the European eel's swimming backward in Section 5. The difference between simulated and experimented data at $f=1.85\text{Hz}$ and $f=1.67\text{Hz}$ are larger, and it is caused by the affection between the links, and the affection increases when frequency is higher.

V. CONCLUSIONS

The swimming backward motion of biomimetic carangiform robotic fish is presented in this paper. Based on the biomimetic carangiform robotic fish, a dynamical and kinematical model is given to analyze the propulsion produced by the undulation of the multi-link tail. The difference between the anguilliform mode and carangiform mode is discussed. A method for carangiform robotic fish swimming backward is proposed. Simulations and Experiments verified the feasibility of the proposed method in the application of robotic fish.

REFERENCES

- [1] M. J. Lighthill, "Large-amplitude elongated-body theory of fish locomotion," *Proc. R. Soc. Lond. Ser. B*, 1971, Vol.179, 125-138
- [2] M. J. Lighthill, "Note on the swimming of slender fish," *J. Fluid Mech.* vol. 9, pp.305-317, 1960. 18
- [3] T. Y. Wu, "Swimming of a waving plate," *J. Fluid Mech.* 1961, Vol.10, 321-344
- [4] M. S. Triantafyllou and G. S. Triantafyllou, "An efficient swimming machine," *Sci. Amer.*, Vol. 272, no. 3, Mar. 1995, pp. 64-70.
- [5] B. Tong, "Propulsive mechanism of fish's undulatory motion," *Mechanics In Engineering*, 22: pp. 69-74. 2000.
- [6] B. Tong, "Propulsive mechanism of fish's undulatory motion," *Mechanics In Engineering*, 2000, 22: 69-74. (in Chinese)
- [7] C. M. Breder, "The locomotion of fishes," *Zoologica*, Vol. 4, 1926, pp. 159-256.
- [8] K. A. McIsaac and J. P. Ostrowski, "Motion Planning for Anguilliform Locomotion," *IEEE Transaction on Robotics and Automation*, Vol.19, Issue 4, Aug. 2003 Page(s):637-652
- [9] K. H. Low, "Locomotion Consideration and Implementation of Robotic Fish with Modular Undulating Fins: II. Analysis and Experimental Study," *IROS 2006*, Beijing, China, Oct 2006.
- [10] N. Kato, H. Liu and H. Morikawa "Biology-inspired Precision Maneuvering of Underwater Vehicles Part 3, " *Int. J. of Offshore and Polar Engineering*, 2005, Vol. 15, No. 2, pp. 81-87
- [11] C. Zhou, L. Wang, Z. Cao, S. Wang and M. Tan, "Design and Control of Biomimetic Robot Fish FAC-I," in *Bio-mechanisms of Swimming and Flying* (Springer, Eds. N. Kato and S. Kamimura), 2006, pp.247-258
- [12] C. Zhou, Z. Cao, S. Wang and M. Tan, "The Posture Control and 3-D Locomotion Implementation of Biomimetic Robot Fish," *IEEE IROS*, 2006, pp. 5406-5411
- [13] K. A. Morgansen, V. Duindam, Richard J. Mason, et al. "Nonlinear control methods for planar carangiform robot fish locomotion." *IEEE ICRA 2001*, pp. 427-434.
- [14] J. Liu and H. Hu, "Building a 3D simulator for autonomous navigation of robotic fishes," *IEEE IROS 2004*, pp. 613-618
- [15] J. Yu, L. Wang and M. Tan, "Geometric Optimization of Relative Link Lengths for Biomimetic Robotic Fish," *IEEE Transactions on Robotics*, Vol.23, Issue 2, Apr. 2007, pp:382 - 386
- [16] M. S. Triantafyllou and G. S. Triantafyllou, "An efficient swimming machine," *Sci. Amer.*, Vol. 272, no. 3, Mar. 1995, pp. 64-70.
- [17] D'Août K. and Aerts P. "A kinematic comparison of forward and backward swimming in the eel (*Anguilla anguilla*)," *J. Exp. Biol.* 1999. 202: 1511-1521.
- [18] Shape Effects on Drag [Online]. Available: <http://wright.nasa.gov/airplane/shaped.html>